6-*S*-Cysteinyl Flavin Mononucleotide-Containing Histamine Dehydrogenase from *Nocardioides simplex*: Molecular Cloning, Sequencing, Overexpression, and Characterization of Redox Centers of Enzyme†

Nobutaka Fujieda, Atsuko Satoh, Noriaki Tsuse, Kenji Kano,* and Tokuji Ikeda

Division of Applied Life Sciences, Graduate School of Agriculture, Kyoto University, Sakyo-ku, Kyoto 606-8502, Japan

Received May 10, 2004; Revised Manuscript Received June 14, 2004

ABSTRACT: Histamine dehydrogenase from *Nocardioides simplex* is a homodimeric enzyme and catalyzes oxidative deamination of histamine. The gene encoding this enzyme has been sequenced and cloned by polymerase chain reactions and overexpressed in *Escherichia coli*. The sequence of the complete open reading frame, 2073 bp coding for a protein of 690 amino acids, was determined on both strands. The amino acid sequence of histamine dehydrogenase is closely related to those of trimethylamine dehydrogenase and dimethylamine dehydrogenase containing an unusual covalently bound flavin mononucleotide, 6-*S*-cysteinyl-flavin mononucleotide, and one 4Fe−4S cluster as redox active cofactors in each subunit of the homodimer. The presence of the identical redox cofactors in histamine dehydrogenase has been confirmed by sequence alignment analysis, mass spectral analysis, UV−vis and EPR spectroscopy, and chemical analysis of iron and acid-labile sulfur. These results suggest that the structure of histamine dehydrogenase in the vicinity of the two redox centers is almost identical to that of trimethylamine dehydrogenase as a whole. The structure modeling study, however, demonstrated that a putative substrate-binding cavity in histamine dehydrogenase is quite distinct from that of trimethylamine dehydrogenase.

Histamine is one of the most significant bioactive amines, playing a key role in the regulation of several physiological processes, and is recognized in high specificity by various proteins. Although several efforts have been devoted to understanding the mode of its binding with various proteins from physiological and pharmacological viewpoints (*1*), details remain still obscure. Recently, histamine dehydrogenase (HmDH)[1] has been discovered from *Nocardioides simplex*, one of Gram-positive actinobacteria (*2*, *3*). The enzyme is a homodimer and highly specific to histamine and catalyzes the oxidative deamination of histamine to imidazole acetaldehyde where A and AH_2 are a two-electron acceptor

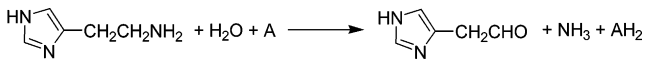

(1)

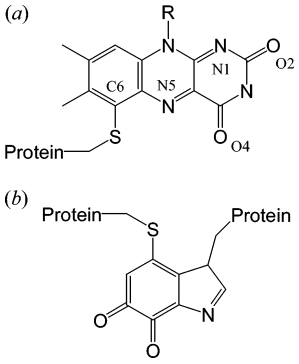

FIGURE 1: Structures of (a) 6-*S*-cysteinyl-flavin mononucleotide and (b) cysteine tryptophylquinone.

(or two moles of one-electron acceptor) and its reduced form, respectively. It was suggested that HmDH contained a covalently bound organic cofactor, which was expected to be a quinone-like compound on the basis of its absorption spectra and the positive staining in quinone-dependent redox cycling (*2*).

Two kinds of quinoprotein primary-amine dehydrogenases have been discovered to date from some Gram-negative bacteria. These enzymes catalyze the following reaction:

$$RCH_2NH_2 + H_2O + A \rightarrow RCHO + NH_3 + AH_2 \quad (2)$$

One group includes methylamine dehydrogenase from *Paracoccus denitrificans* (*4*) and aromatic amine dehydrogenase from *Alcaligenes faecalis* (*5*). These enzymes possess $\alpha_2\beta_2$ subunit structure and one covalently bound tryptophan tryptophylquinone as a prosthetic group in each β subunit

† This work was financially supported by Grants-in-Aids for Scientific Research from the Ministry of Education, Culture, Sports, Science, and Technology of Japan (MECSSTJ), Casio Science Promotion Foundation to K.K. and T.I., Research Fellowships of Japan Society for the Promotion of Science for Young Scientists to A.S., and COE for Microbial-Process Development Pioneering Future Production Systems (COE program of MECSSTJ).

* To whom correspondence should be addressed. Tel: +81-75-753-6393. Fax: +81-75-753-6456. E-mail: kkano@kais.kyoto-u.ac.jp.

[1] Abbreviations: HmDH, histamine dehydrogenase from *Nocardioides simplex* NBRC 12069; *N. simplex*, *Nocardioides simplex*; TMADH, trimethylamine dehydrogenase; DMADH, dimethylamine dehydrogenase; FMN, flavin mononucleotide; FAD, flavin adenine dinucleotide; CTQ, cysteine tryptophyl quinone; ETF, electron-transfer flavoprotein; EPR, electron spin paramagnetic resonance spectroscopy; ESMS, electrospray ionization mass spectroscopy; TAIL-PCR, thermal asymmetric interlaced PCR.

10.1021/bi049061q CCC: $27.50
Published on Web 07/23/2004

(*6*, *7*). The other group includes quinohemoprotein amine dehydrogenase (QH-AmDH) from *Pseudomonas putida* (*8*) and *Paracoccus denitrificans* (*9*). QH-AmDH consists of a heterotrimer and bears two hemes *c* in the largest subunit and one covalently bound cysteine tryptophylquinone (CTQ) in the smallest subunit as the redox active prosthetic group (Figure 1b) (*10*, *11*).

Another class of amine dehydrogenases is trimethylamine dehydrogenase (TMADH) from *Methylophilus methylotrophus* W_3A_1 and *Hyphomicrobium X* (*12*) and dimethylamine dehydrogenase (DMADH) from *Hyphomicrobium X* (*13*). These enzymes catalyze oxidative N-demethylation of tertiary and secondary amines:

$$RN(CH_3)_2 + H_2O + A \rightarrow RNH(CH_3) + HCHO + AH_2 \quad (R = CH_3 \text{ or } H) \quad (3)$$

TMADH and DMADH have a homodimeric structure; each subunit bears a 4Fe−4S cluster (*14*) and an unusual covalently bound flavin mononucleotide (FMN), 6-*S*-cysteinyl-FMN (Figure 1a) (*15*−*17*). The primary structures of these two enzymes have been determined and are in a close relationship (63% identical) with each other, indicating that the enzymes are structurally homologous (*18*, *19*). The crystal structure of TMADH has been solved at 2.4 Å resolution (*20*). Crystal analyses of TMADH soaked in a substrate inhibitor tetramethylammonium chloride solution or in a substrate trimethylamine solution revealed that these quaternary and tertiary ammonium ligands are accommodated in an aromatic bowl consisting of three residues: Tyr60, Trp264, and Trp355 (TMADH numbering) (*21*). The molecular modeling analysis of DMADH based on the crystal structure of TMADH indicated that both active site architectures are almost identical (*22*). The model demonstrated that a single amino acid substitution (Tyr60 → Gln60) is responsible for the switch in substrate specificity in these two amine dehydrogenases. Several TMADH mutants were isolated by conventional site-directed mutagenesis, and kinetic study with the mutants revealed some reasons why DMADH binds secondary alkylammonium ion preferentially over tertiary alkylammonium ion (*23*).

In this study, we have clarified the primary structure of HmDH from *N. simplex* by PCR methods and overexpressed HmDH successfully in *Escherichia coli*. The amino acid sequence is highly correlated with those of TMADH and DMADH. This result suggests the presence of 6-*S*-cysteinyl-FMN and 4Fe−4S cluster as the redox centers in HmDH, and the expectation was verified by chemical and spectroscopic analyses. Moreover, sequence alignment study of the three 6-*S*-cysteinyl-FMN-containg enzymes and molecular modeling study based on the crystal coordinates of TMADH were performed for better understanding of the catalytic center, particularly the substrate binding site cavity.

EXPERIMENTAL PROCEDURES

Enzyme Purification. The culture conditions of *N. simplex* NBRC 12069 and the purification of HmDH were almost the same as described in a previous report (*2*) with some modifications. The cell-free extract was charged on a DEAE-Sepharose column (Amersham), equilibrated with 0.01 M potassium phosphate, pH 7.5, and eluted with a linear gradient of the buffer containing 0−0.5 M NaCl. The final purification step was accomplished on a column of Hiload 26/60 Superdex 200 pg (Amersham) equilibrated with 0.05 M sodium phosphate, pH 7.5, containing 0.15 M NaCl. QH-AmDH from *P. denitrificans* was purified as described in the literature (*9*) and used as a reference enzyme in electron spin paramagnetic resonance spectroscopy (EPR).

Protein Sequencing and Mass Spectroscopy of HmDH. Automated Edman degradation was performed on a protein sequencer Procise 492 (Applied Biosystems), and electrospray ionization mass spectroscopy (ESMS) was done on a quadrupole mass spectrometer API 165 (PerkinElmer Sciex). For these measurements, HmDH samples were further purified and desalted using an Asahipak C4P C_4 reverse-phase column (Shodex) pre-equilibrated with solvent A (0.1% trifluoroacetic acid, H_2O) and eluted with linear gradient of 5−80% solvent B (0.08% trifluoroacetic acid, acetonitrile) over 30 min at 40 °C. The highly purified sample was analyzed as soon as possible (within 24 h) with ESMS spectroscopy. To obtain internal amino acid sequences, HmDH was precipitated at 0 °C by addition of trichloroacetic acid to a final concentration of 5% (w/v). After centrifugation, the precipitate was resuspended in 0.1 M Tris-HCl buffer at pH 8.1. Trypsin and chymotrypsin were added in a ratio of 1:50 (w/w) against HmDH. The tryptic and chymotryptic peptides were separated on a Symmetry 300 Å C_{18} reverse-phase column (Waters Co.).

Cloning and Sequence Determination of the hmd Gene. Chromosomal DNA from *N. simplex* was prepared with an AquaPure Genomic DNA Isolation Kit (Bio-rad). To clone and sequence the *hmd* gene, degenerated oligonucleotide primers were designed based on the N-terminal and the internal amino acid sequences as (5′-CGA(C/T)GT(C/G/T)-CT(C/G)TTCGA(A/G)CC(A/T/G/C)GT(C/G/ T)CAGATC-GG-3′ and 5′-CTTGTT(A/C/G)GG(C/G)AGGAA(A/T/G/C)-GG(A/ G)TC-3′). An about 1 kbp portion of the *hmd* gene was amplified from genomic DNA of *N. simplex* by polymerase chain reaction (PCR) with these degenerated primers and Taq polymerase (Promega). The conditions of the amplification (30 cycles) were as follows: denaturation 94 °C (30 s), annealing 55 °C (30 s), and extension 73 °C (90 s). After purification on agarose gels, the fragments were ligated in pGEM-T EASY Vector, a TA cloning vector, for preliminary sequencing. Recommendations of the manufacturer (Promega) are followed in all manipulations of the plasmid and conditions for ligation. *E. coli* JM109 cells were transformed with the ligated plasmid according to the literature (*24*). Three fragments of about 0.4, 0.7, and 2.5 kbp were amplified by the thermal asymmetric interlaced PCR (TAIL-PCR) method with a shorter arbitrary degenerated primer (5′-(A/T/G/C)TCGA(C/G)T(A/T)T(C/G)G(A/T)-GTT-3′) and KOD Dash polymerase (Toyobo). Other details were described in the literature (*25*, *26*). These fragments were also subcloned into pGEM-T EASY Vector and sequenced. On the basis of the sequences of the cloned fragments, two primers (5′-AGCTGACCTTCGAGGCCT-TCACGCT-3′ and 5′-GACGAGTCCGCTGAACGGGAT-3′) were synthesized and used to amplify the complete *hmd* gene from chromosomal DNA with high-fidelity KOD plus DNA polymerase (Toyobo) over 25 step-down cycles (*27*). The DNA fragments were purified from agarose gels and

directly subjected to DNA sequence analysis to make sure of the final sequence (or exclude all PCR errors).

All DNA sequence analyses were performed by cycle sequencing techniques using a RISA-384 DNA sequencer. To confirm the DNA sequence of the entire gene and the expression construct pEThmd, DNA sequencing was performed on both strands using synthetic primers that were designed to bind at about 0.4 kbp intervals along the length of the gene. The *N. simplex hmd* sequence has been deposited in EMBL/GenBank/DDBJ under accession number AB120626. All oligonucleotides were purchased from Hokkaido System Science Co. The amino acid residues in alignment analysis are in HmDH numbering, and the initiating methionine is assigned as residue 0 unless otherwise stated.

Expression and Analysis of Recombinant HmDH. For recombinant expression in *E. coli*, the *hmd* gene was amplified with KOD plus DNA polymerase using two primers (5′-catATGACCGAGCAGCCCGCCGT-3′ and 5′-aagcttCAGAGTTGCGCCTCACGCCAG-3′; the residues printed in capital letters being complementary to the template sequence) from chromosomal DNA in the same manner as described previously. The fragment was ligated into pGEM-T EASY Vector and sequenced. Then, this plasmid was digested with *Nde*I and *Hind*III (the *Nde*I and *Hind*III recognition sites being underlined in the sequences of the two primers) and inserted into pET-26b(+) (Novagen) to yield the expression construct pEThmd. The *E. coli* strain Rosetta (DE3) (Novagen) was transformed with pEThmd and grown in Luria−Bertani medium containing 0.1% (W/V) glucose at 30 °C. In the late exponential phase, induction of recombinant protein expression was afforded by addition of isopropyl β-D-thiogalactoside (1 mM). Cells were harvested by centrifugation and disrupted by sonication in 0.01 M potassium phosphate buffer pH 7.5. Cell lysates were separated on SDS/PAGE and visualized by staining with Coomassie brilliant blue R250. HmDH activity in the soluble fraction of the cell lysates was assayed spectrophotometrically with phenazine methosulfate and 2,6-dichloroindophenol as described in the literature (*2*).

Isolation and Analysis of the Cofactor-Containing Peptide. The cofactor-containing peptide was prepared as follows. HmDH was first reductively carboxymethyled; HmDH (1 mg/ml) was reduced with 2 mg/mL dithiothreitol for 5 h in 100 mM Tris-HCl buffer (pH 8.0) containing 6 M guanidine hydrochloride under Ar gas stream. The reduced sample was treated with a freshly prepared solution of iodoacetic acid (5 mg/mL) for 30 min. After concentration to about 10 mg/mL, the sample was digested for 24 h at 37 °C with lysyl endopeptidase (Wako) (0.4 mg/mL peptidase solution in 100 mM Tris-HCl pH 9.2). The cofactor-containing peptide was separated on a Symmetry 300 Å C_{18} column equilibrated with solvent A. The elution was in a linear gradient from 5 to 30% of solvent B over 60 min and then a subsequent gradient to 60% over 30 min at 40 °C. The cofactor-containing peptide fraction was lyophilized. The sample was dissolved in distilled water and 0.1 M potassium phosphate buffer pH 7.0 for Edman degradation analysis and UV−vis absorption spectroscopy, respectively. For ESMS analysis, however, the sample was dissolved in solvent C (0.2% acetic acid, 50% acetonitrile, and 50% H_2O) or solvent D (0.1% trifluoroacetic acid, 50% acetonitrile, and 50% H_2O).

Other Analytical Methods. Protein concentrations were determined based on both Biuret method (*28*) and modified Lowry method with a DC Protein Assay Kit (Bio-rad) using bovine serum albumin as a standard. Iron and acid-labile sulfur were determined by the published procedures (*29*, *30*). UV−vis absorption spectra were recorded on a Shimadzu UV-2500PC spectrophotometer. EPR spectroscopy was performed as described in a previous paper (*9*).

RESULTS

Identification of hmd Gene Encoding Histamine Dehydrogenase. N-Terminal sequence analysis of the intact HmDH and of its internal peptide obtained by trypsin and chymotrypsin digestion revealed small regions of the sequence to be determined as N-terminal: TEQPAVAAPYDVLFEPVQIGPFTT*NRFY and the internal peptide: IADPFLPNK (the amino acid residue indicated by asterisk could not be identified by Edman degradation analysis). PCR with the corresponding degenerated primers yielded a 976 bp fragment. On the basis of the DNA sequence information on this fragment, two sets of three primers were synthesized for TAIL-PCR, which yielded two fragments of 355 and 763 bp in length. The sequence analysis revealed that the former fragment included the complete 5′-region of the *hmd* gene. However, the latter sequence obviously lacked the 3′-end of the *hmd* gene. The third try of TAIL-PCR was to use the other set of three primers, which resulted in the generation of about 2.5 kb amplicon including the missing part of the gene. On the basis of the sequence of the four PCR fragments, two primers were designed to amplify the complete *hmd* gene as one contiguous fragment. This amplification using high-fidelity KOD plus DNA polymerase yielded a 2322 bp fragment. The independently amplified fragments were directly subjected to DNA sequence analysis at least three times. No conflict was observed on comparison of the resulting sequences, indicating the precise determination of the *hmd* gene sequence.

An open reading frame was identified in the fragment, which is 2073 bp in length and encodes a protein of 690 amino acids (including the N-terminal methionine residue, which is absent when HmDH is expressed in *N. simplex*) (Figure 2) with a calculated molecular weight of 75 608 for an apoenzyme subunit, which is close to the reported values of the holoenzyme subunit by about 84 kDa based on gel chromatographic and SDS/PAGE analyses (*2*). The *hmd* gene comprises 13.1% T, 36.1% C, 15.8% A, and 35.0% G and has high GC contents as seen in many actinobacteria such as *Streptomyces* species. The analysis of the DNA sequence flanking the *hmd* gene failed to reveal sequence elements that would suggest the presence of promotor sequences. However, there is a putative stem-loop structure at the 3′-end of the gene covering nucleotides 2097−2138: (5′-GCGCCCGGtACGGCGGCAGgggaCTGCCGCCGTgCCGGGCGC-3′; residues printed in capital letters corresponding to a putative stem-loop structure), which seems to act as a transcription termination signal. There is also a putative ribosome-binding site at the 5′-end of the gene covering nucleotides from −10 to −13 (5′-AGGA-3′). The two polypeptide sequences determined chemically are exactly identical with the corresponding portions of the deduced *hmd* amino acid sequence, respectively.

```
HMDH     MTEQPAVAAPYDVLFEPVQIGPFTTKNRFYQVPHCNGMGYRDPSAQASMRKIKAEGGWSVVCTEQVEIHATSDIAPFIEL  79
TMADH    MARDP----KHDILFEPIQIGPKTLRNRFYQVPHCIGAGSDKPGFQSAHRSVKAEGGWAALNTEYCSINPESDDTHRLSA  75
DMADH    MARDP----RFDILFTPLKLGSKTIRNRFYQVPHCNGAGTNSPGMNMAHRGIKAEGGWGAVNTECCSIHPECDDTLRITA  75
         *   *      * ** *   *  *  ********* * *   *      *  ******    **   *    *

HMDH     RIWDDQDLPALKRIADAIHEGGGLAGIELAHNGMNAPNQLSRETPLGPGHLPVAPDTIAP----IQARAMTKQDIDDLRR 155
TMADH    RIWDEGDVRNLKAMTDEVHKYGALAGVELWYGGAHAPNMESRATPRGPSQYASEFETLS------YCKEMDLSDIAQVQQ 149
DMADH    RIWDQGDMRNLRAMVDHVHSHGSLAGCELFYGGPHAPAIESRTISRGPSQYNSEFATVPGCPGFTYNHEADIDELERLQQ 155
         ****  *   *    *  *  * *** **   *  **   **    **        *

HMDH     WHRNAVRRSIEAGYDIVYVYGAHGYSGVHHFLSKRYNQRTDEYGGSLENRMRLLRELLEDTLDECAGRAAVACRITVEEE 235
TMADH    FYVDAAKRSRDAGFDIVYVYGAHSYL-PLQFLNPYYNKRTDKYGGSLENRARFWLETLEKVKHAVGSDCAIATRFGVDTV 228
DMADH    QYVDAALRARDTGFDLVNVYGAHAYG-PMQWLNPYYNRRTDKYGGSFDNRARFWIETLEKIRRAVNDDVALVTRCATDTL 234
           *  *    * * * ***** *     *   ** *** ****  ** *   * **         *   *

HMDH     IDGGITREDIEG--VLRELGELPDLWDFAMG---SWEGDSVTSRFAPEGRQEEFVAGLKKLTTKPVVGVGRFTSPDAMVR 310
TMADH    YGPGQIEAEVDGQKFVEMADSLVDMWDITIGDIAEWGEDAGPSRFYQQGHTIPWVKLVKQVSKKPVLGVGRYTDPEKMIE 308
DMADH    YGTKGVELTEDGLRFIELASPYLDIWDVNIGDIAEWGEDAGPSRFYPIAHENDWIRHIKQATNKPVVGVGRYYDPEKMLQ 314
                 *           * **   *    *  *   ***           *     *** ****   *  *

HMDH     QIKAGILDLIGAARPSIADPFLPNKIRDGRLNLIRECIGCNICVS-GDLTMSPIRCTQNPSMGEEWRRGWHPERIRAKES 389
TMADH    IVTKGYADIIGCARPSIADPFLPQKVEQGRYDDIRVCIGCNVCISRWEIGGPPMICTQNATAGEEYRRGWHPEKFRQTKN 388
DMADH    VIKAGIIDIIGAARPSIADPWLPRKIDEGRVDDIRTCIGCNVCISRIEMGGVPFICTQNATAGEEYRRGWHPEKFEPKKS 394
           *  * ** ******** ** *   **   ** ***** * *       *  ****   *** *******

HMDH     DARVLVVGAGPSGLEAARALGVRGYDVVLAEAGRDLGGRVTQESALPGLSAWGRVKEYREAVLAELPN-----VEIYRES 464
TMADH    KDSVLIVGAGPSGSEAARVLMESGYTVHLTDTAEKIGGHLNQVAALPGLGEWSYHRDYRETQITKLLKKNKESQLALGQK 468
DMADH    DHDVLIVGAGPAGSECARVLMERGYTVHLVDTREKTGGYVNDVATLPGLGEWSFHRDYRQTQLEKLLKKNPECQIALKQK 474
            ** ***** * * ** *   ** * *       **       ****  *     **      *

HMDH     PMTGDDIVEFGFEHVITATGATWRTDGVARFHTTALPIAEG--MQVLGPDDLFAGRLPDGKKVVVYDDDHYYLGGVVAEL 542
TMADH    PMTADDVLQYGADKVIIATGARWNTDGTNCLTHDPIPGADASLPDQLTPEQVMDGKKKIGKRVVILNADTYFMAPSLAEK 548
DMADH    PMTADDILQYGASRVVIATGAKWSTTGVNHRTHEPIPGADASLPHVLTPEQVYEGKKAVGKRVMIINYDAYYTAPSLAEK 554
         *** **    *   *  **** * * *       * *       *  *     *    ** *     * *      **

HMDH     LAQKGYEVSIVTPGAQVSSWTNNTFEVNRIQRRLIENGIARVTDHAVVAVGAGGVTVRDTYAS----------------- 605
TMADH    LATAGHEVTIVS-GVHLANYMHFTLEYPNMMRRLHELHVEELGDHFCSRIEPGRMEIYNIWGDGSKRTYRGPGVSPRDAN 627
DMADH    FARAGHDVTVAT-VCGLGAYMEYTLEGANMQRLIHELGIKVLGETGCSRVEQGRVELFNIWGEGYKRSYKGAGQLPRNEN 633
          *  *  *               * *     *   *             *

HMDH     -IERELECDAVVMVTARLPREELYLDLVARR---DAGEIASVRGIGDAWAPGTIAAAVWSGRRAAEEFDAVLPSNDEVPF 681
TMADH    TSHRWIEFDSLVLVTGRHSECTLWNELKARESEWAENDIKGIYLIGDAEAPRLIADATFTGHRVAREIEEANP-QIAIPY 706
DMADH    TSHEWHECDTVILVTSRRSEDTLYRELKARKGEWEANGITNVFVIGDAESPRIIADATFDGHRLAREIEDADP-QHQKPY 712
           * *    ** *     *   * **        *     ****  *  ** *   * * * *     *     *

HMDH     RREVTQLA---------------- 689
TMADH    KRETIAWGTPHMPGGNFKIEYKV 729
DMADH    KREQRAWGTAYNPDENPDLVWRV 735
```

FIGURE 2: Sequence alignment of HmDH from *N. simplex* and related dehydrogenases. The present alignment was performed using the CLUSTAL W routine of the GenomeNet. All the amino acid sequences of trimethylamine dehydrogenase from *M. methylotrophus* (W_3A_1) and dimethylamine dehydrogenase from *Hyphomicrobium X* were simultaneously compared with the histamine dehydrogenase sequence from *N. simplex*. The whole identities are 40.0 and 39.4%, respectively, and the sequences asterisked above are common residues. Residues that are shaded in gray are components of the active site and cysteines covalently linked to the cofactors, and those in black are the substrate-binding sites.

Recombinant expression of the wild-type HmDH was achieved using bacterial expression vector pET-26b(+). The expression vector, designated pEThmd, brings the *hmd* gene under the control of the T7 promoter. Transformation of the vector into *E. coli* strain Rosetta (DE3) containing T7 RNA polymerase and induction with isopropyl β-D-thiogalactoside for 3 h resulted in the expression of a protein in a high yield with a molecular mass close to that of native HmDH (Figure 3). The cell lysates exhibited strong HmDH activity. Without the induction treatment, however, *E. coli* strain Rosetta (DE3) with pEThmd did not show any HmDH activity. These results indicate that the T7 promoter functions properly and that the *hmd* gene obtained in this study encodes HmDH exactly.

Redox Active Prosthetic Groups of HmDH. It was suggested that HmDH would contain a covalently bound quinone-like organic cofactor, but details remained unknown (*2*). Comparisons of the deduced *hmd* amino acid sequence with the sequences deposited in the protein and DNA databases using the program FASTA revealed high similarity with TMADH from *Methylophilus methylotrophus* W_3A_1 and DMADH from *Hyphomicrobium X* (Figure 2). TMADH and DMADH contain a covalently bound flavin coenzyme, 6-*S*-cysteinyl-FMN, and also a tetrameric 4Fe−4S cluster as the redox active prosthetic groups (*14*−*17*). Alignment analysis of these two proteins with HmDH reveals that a 4Fe−4S cluster binding motif is conserved in a portion of the amino acid residues from 346 to 355 including three cysteine residues (*31*). The fourth cysteine for the cluster formation is also highly conserved as Cys365, indicating that the HmDH subunit has one single iron−sulfur center [4Fe−4S].

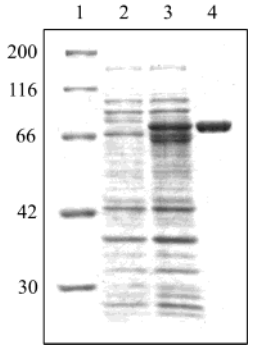

FIGURE 3: SDS/PAGE analysis of the expression of the *hmd* gene. Samples were separated by SDS/PAGE in a 10% polyacrylamide gel and stained with Coomassie brilliant blue R250. Lane 1, molecular mass markers: myosin (200 kDa), β-galactosidase (116 kDa), bovine serum albumin (66.3 kDa), aldolase (42.4 kDa), and carbonic anhydrase (30.0 kDa); lane 2, *E. coli* strain Rosetta (DE3) containing the pEThmd expression construct without induction; lane 3, *E. coli* strain Rosetta (DE3) containing the pEThmd expression construct after induction; and lane 4, histamine dehydrogenase purified from *N. simplex*.

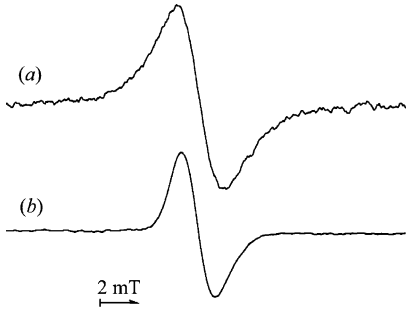

FIGURE 4: EPR spectra of the substrate-reduced state of (a) HmDH from *N. simplex* and (b) QH-AmDH from *P. denitrificans.* HmDH was reduced with excess amounts of histamine, while QH-AmDH was partially reduced with small amounts of *n*-butylamine in potassium phosphate buffer at pH 7.0 and at room temperature.

Another cysteine residue to form covalent 6-*S*-cysteinyl-FMN is also conserved as Cys34 (*32*). Furthermore, two amino acid residues, His33 and Arg229, were conserved, which have been reported to play important roles in the posttranslational formation of the cysteinyl bond as its reaction base (*33*) and as the stabilizer to neutralize negative charges on the N1/O2 atoms of the flavin (*34*), respectively (Figure 1). These results suggest that HmDH has two redox active prosthetic groups as in the case of TMADH and DMADH.

Determination of the Two Redox Active Prosthetic Groups. HmDH prepared in high purity from *N. simplex* was analyzed on ESMS. Considering the experimental errors of the ESMS measurements, the multiply charged ion peaks were assigned to a protein with a molecular weight of $(75.9 \pm 0.1) \times 10^3$ (standard deviation from five determinations). The value is larger by ca. 0.4×10^3 than the apoenzyme subunit molecular weight (75 477) calculated from the *hmd* sequence. The difference is in good agreement with the additional mass for 6-*S*-cysteinyl-FMN (molecular weight of FMN: 456) generated posttranslationally. The 4Fe−4S iron−sulfur cluster must have been liberated from denaturated HmDH under the acidic conditions (pH ≅ 1) of the HPLC step.

HmDH gave a strong EPR spectrum at $g \cong 2$ upon the reduction with excess amounts of histamine at pH 7.0 at room temperature (Figure 4a), where a two-electron reduction of the enzyme must take place. The total line width of the EPR spectrum was ca. 6.0 mT, indicating the generation of a quinone-like organic radical. However, the line width was larger than that observed for CTQ-containing QH-AmDH from *P. denitrificans* (4.5 mT, Figure 4b). This difference is interpretable by considering the coupling of the nitrogen atom(s) of 6-*S*-cysteinyl-FMN in HmDH. The EPR spectrum disappeared when HmDH was reduced with dithionite, indicating further reduction (most probably totally three-electron reduction) of HmDH. The generation of the flavosemiquinone on substrate reduction (two-electron reduction) suggests an intraprotein single-electron transfer from the fully reduced flavin to a single-electron acceptor in HmDH.

To identify the covalently bound organic cofactor, HmDH was subjected to reductive carboxymethylation and subsequently digested with lysyl endopeptidase. The cofactor-containing peptide was purified by HPLC. The chromophore-containing peptide was eluted as a practically single peak. The absorption spectrum was very unique (Figure 5). Automated Edman degradation of this peptide identified the

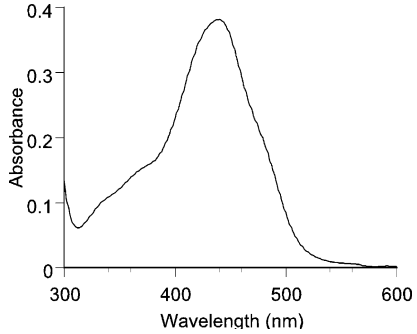

FIGURE 5: UV−vis absorption spectrum of the cofactor-containing peptide in HmDH. The absorption spectrum of the purified peptide was recorded in 0.1 M potassium phosphate buffer pH 7.0.

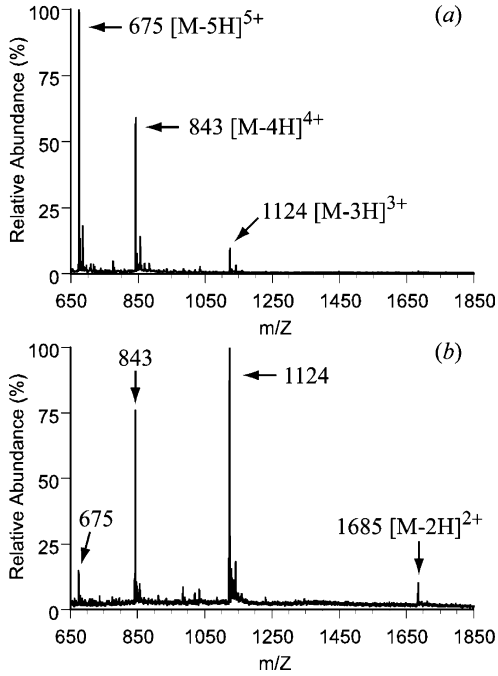

FIGURE 6: Positive mode ESMS spectrum of the cofactor-containing peptide in HmDH. The lyophilized sample was dissolved in solvent C (ca. 5 μM) containing 0.2% acetic acid (a) and solvent D containing 0.1% trifluoroacetic acid (b) just before ESMS analysis.

following sequence: NRFYQVPH*NGMGYRDPSAQASMRK, which corresponds to residues 26−50 in the sequence of HmDH. The amino acid replaced with the asterisk was not identified in Edman degradation analysis and can be reasonably assigned to the site of the modified cysteine. This peptide was also subjected to ESMS analysis. When solvent C was used for the sample preparation (see Experimental Procedures), the three major multiply charged ions were observed at *m*/*z* of 675, 843, and 1124 (Figure 6a). These peaks were assigned to $[M - 5H]^{5+}$, $[M - 4H]^{4+}$, and $[M - 3H]^{3+}$, respectively. Another ion peak of *m*/*z* 1685 to be assigned to $[M - 2H]^{2+}$ was also observed when solvent D was used, although the total intensity of ion peaks decreased (Figure 6b). The signals to be assigned to $[M - H]^{+}$ and $[M - 6H]^{6+}$ could not be observed under the present conditions. As a result, the molecular weight of this peptide was determined by deconvolution to be 3368.6 ± 0.2 (standard deviation from eight determinations), which is identical with the value (3368.6) calculated for the corresponding sequence having 6-*S*-cysteinyl FMN. These data verify that FMN is covalently bound to this peptide at Cys34.

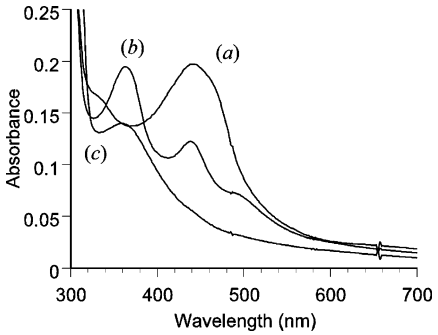

FIGURE 7: UV−vis absorption spectra of (a) the fully oxidized form, (b) substrate-reduced form, and (c) dithionite-reduced form of HmDH at pH 8.5. Substrate-reduced form was prepared by addition the substrate histamine to HmDH at a final concentration of 1 mM. Dithionite-reduced form was prepared by adding solid dithionite to the substrate reduced enzyme solution. A spectrum almost identical with spectrum c was obtained when HmDH was directly reduced with excess dithonite.

Covalently linked forms of flavins occur more frequently in flavin adenine dinucleotide (FAD)-dependent enzymes than that in FMN-dependent ones. Covalently bound FAD is usually linked to the histidine or cysteine residue at the 8α-methyl group of the isoalloxazine ring (*35*), and those absorption spectra are almost identical with those of noncovalent FADs (*36*). The peptide obtained in this experiment shows a spectrum with a peak at 440 nm and a shoulder at 480 nm (Figure 5), which is distinguished from that of FAD. The absorption spectrum has, rather, a very close similarity with that of 6-*S*-cysteinyl FMN in denaturated TMADH (*32*).

Another important point is to verify the presence of a ferredoxin-like 4Fe−4S cluster, which is included in TMADH and DMADH. Iron and acid-labile sulfur in HmDH were analyzed to be 7.6 and 8.1 mol per mol of HmDH, respectively. The absorption spectra of HmDH in the oxidized forms and substrate-reduced forms (Figure 7, spectra a and b) were almost identical with the corresponding spectra of TMADH and DMADH (*17*, *37*, *38*). The molar extinction coefficient of the fully oxidized HmDH was determined to be 48.3 mM^{-1} cm^{-1} at 442 nm on the basis of protein determination. This value is close to that of TMADH (52.3 mM^{-1} cm^{-1} at 443 nm) and DMADH (49.4 mM^{-1} cm^{-1} at 440 nm) (*39*). Addition of small amounts of solid dithionite to substrate-reduced HmDH (or the oxidized HmDH) caused further reduction of HmDH (Figure 7, spectrum c), indicating the one-electron reduction of flavosemiquinone. From these results, we can safely conclude that HmDH has one covalently bound flavin, 6-*S*-cysteinyl-FMN, and one 4Fe−4S cluster as the redox active groups in each subunit.

Preliminary Characterization of the Catalytic Center. Considering the high conservation in the sequence patterns among HmDH, TMADH, and DMADH, the overall structure and substrate-binding site are likely to be conserved among them. In this regard, the sequence alignment analysis may be allowed, considering the residues that play significant catalytic roles. Actually, many residues in the active site are conserved, for example, Tyr175, His178, Arg229, Trp266, and Asp269 (*34*, *40*, *41*). For better understanding of the catalytic center of HmDH, homology modeling of the three-dimensional structure of HmDH was generated using the SWISS-MODEL server (http://www.expasy.org/swissmod/SWISS-MODEL.html) (*42*). The active site structure is shown in Figure 8a, which was drawn with the program Molscript (*43*). In the theoretical model, the arrangement of the highly conserved residues, Tyr175, His178, Arg229, and Asp269, around the FMN is almost the same as that of TMADH. The hydroxyl group of Tyr175 forms a hydrogen bond with the imidazole side chain of His178. Arg229 and Asp269 are hydrogen bonded to the ribityl 2′- and 3′-hydroxyl groups of the FMN, respectively. On the other hand, Trp266 is also one of the highly conserved residues. However, a significant difference was suggested with respect to the orientation of its side chain between HmDH and TMADH. The indol ring of Trp266 is parallel to the *si*-face of the flavin ring, whereas Trp264 in TMADH hangs over the middle portion of flavin with the approximately perpendicular orientation to each other (Figure 8b). As shown in Figure 2, the residues corresponding to 260−262 in TMADH are missing in HmDH. The loss of the three residues might result in the putative change that Trp266 is directed away from the flavin ring. In addition to the Trp residue described previously, the residues corresponding to Tyr60 and Trp355 in TMADH, which are proposed to be involved in the substrate recognition (*21*, *22*), are replaced with Gln64 and Asp357, respectively. Therefore, the substrate-binding cavity of HmDH appears to be quite different from that of TMADH despite the high sequence identity as a whole.

Furthermore, we attempted to model the binding of substrate, histamine. The imidazole ring of histamine was positioned to occupy the space formed by the aromatic amino acid residues: Trp266 and Phe567. Moreover, Ser270 was found inside the cavity. As a result, the protonated or deprotonated amino group of histamine was lying on the vicinity of the flavin N5. This is located suitably for catalysis: the α-hydrogen of the substrate would be transferred to the N5 of flavin (*41*).

DISCUSSION

HmDH resembles TMADH closely in various aspects such as the molecular weight, the subunit structure, and amino acid sequence homology (40.0% identical), suggesting the homologous three-dimensional structure as a whole. The redox active centers involved in the catalysis and the subsequent electron transfer are identical with those of TMADH (and DMADH). HmDH is the third example of 6-*S*-cysteinyl FMN- and Fe−4S cluster-containing enzymes. The HmDH reaction (eq 1) seems to be somewhat different from those of TMADH and DMADH (eq 3), but all the three enzymes catalyze oxidative N−C bond cleavage, and the reactions are very important in biological systems and essential in the nitrogen cycle on the earth.

Use of the program FASTA with EMBL/GenBank/DDBJ databases has suggested the occurrence of two TMADH-like proteins in *Sinorhizobium meliloti* and *Ralstonia solanacearum*. However, these probable proteins are in higher homology with HmDH (*S. meliloti* (53.1%) and *R. solanacearum* (51.5%)) than with TMADH and DMADH. Actually, *S. meliloti* cultivated under suitable conditions showed HmDH activity (data not shown). Alignment analysis revealed that these probable proteins are very close to HmDH as compared with TMADH and DMADH in view of similarities of amino acid sequence and several gap regions (data not shown). Details of the characterization of the

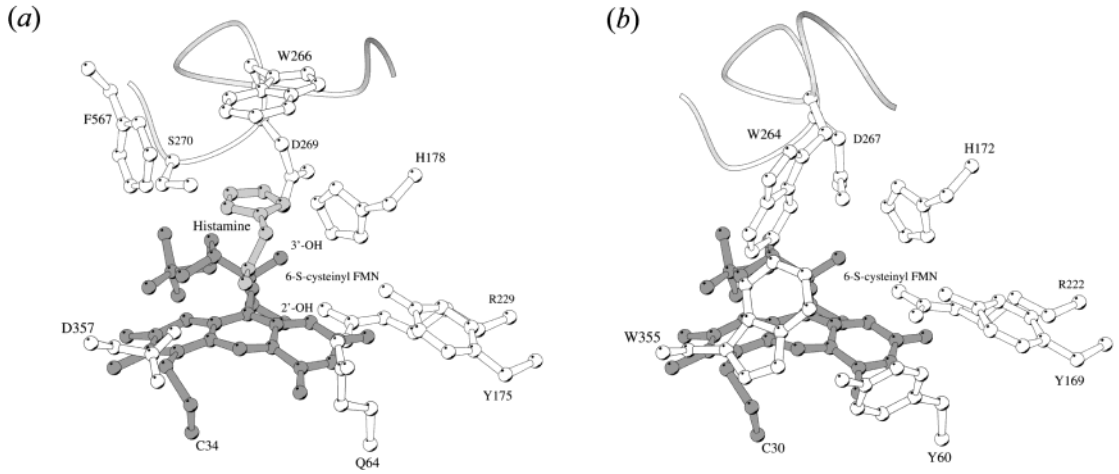

FIGURE 8: Catalytic centers of (a) histamine dehydrogenase model and (b) trimethylamine dehydrogenase. The coordinates used are those of the 2.4 Å structure of trimethylamine dehydrogenase. 6-*S*-Cysteinyl flavin mononucleotide is depicted in dark gray, histamine in light gray, and the amino acid residues in white. The graphic representation was generated using MOLSCRIPT software.

corresponding enzyme from *S. meliloti* will be reported elsewhere in the future.

The oxidoreductases reactions can be divided into the oxidative half-reaction and the reductive half-reaction. The reductive half-reaction of HmDH involves oxidation of the substrate histamine: the two-electron transfer from the substrate to 6-*S*-cysteinyl FMN in the enzyme active site and the subsequent N−C bond cleavage of the substrate. When HmDH was reduced by excess amounts of substrate, HmDH gave a strong EPR signal, which is assigned to the flavosemiquinone radical (Figure 4). The complete three-electron reduction of HmDH was achieved with excess amounts of dithionite, where the EPR spectrum disappeared. Corresponding phenomena were observed in UV−vis absorption spectroscopy (Figure 7). Therefore, a single electron is transferred in the reductive half-reaction from dihydroflavin to the 4Fe−4S center to generate the flavosemiquinone radical and the reduced iron−sulfur center. Similar phenomena have been reported for the reductive half-reaction of TMADH (*37*, *38*). The EPR spectrum of the substrate-reduced enzyme was of particular interest since it showed a complex pattern including a signal with $g \cong 4$ (referred to as the triplet state), indicative of the formation of a spin interacting state of the enzyme after generation of the flavosemiquinone radical and the reduced iron−sulfur center (*37*, *44*−*47*).

The oxidative half-reaction of HmDH should involve two single-electron-transfer events from the reduced 4Fe−4S center to a two-electron acceptor or two single-electron acceptors, coupled with a single-electron transfer from the flavosemiquinone to the 4Fe−4S cluster. Electron transferring flavoprotein (ETF) with FAD is believed to be the native single-electron acceptor of TMADH (*48*). The physiological electron acceptor of HmDH has not been identified yet. However, the physiological electron acceptor of HmDH seems to be different from ETF because Tyr442 in TMADH, which is proposed to play a key role in the complex formation for the interprotein electron transfer (*49*−*52*), is not conserved. Actually, any ETF-like protein could not be found in the purification process of HmDH in *N. simplex* in this study. Rather, production of a F420-like flavin derivative (*53*) was observed in *N. simplex* cells, but F420 did not work as an electron acceptor of HmDH (data not shown). Some single-electron acceptor such as cytochrome *c*, ferredoxin, and azurin might be act as the native electron acceptor of HmDH.

A clear difference between HmDH and TMADH (or DMADH) is the substrate specificity. HmDH is active almost exclusively toward histamine, while low activity is observed for putrescine ($NH_2(CH_2)_4NH_2$) and agmatine ($NH_2(CH_2)_4$-$NHC(NH)NH_2$) (*3*). Trimethylamine and dimethylamine cannot be oxidized at all (data not shown). In TMADH, it has been proposed that the natural substrate trimethylammonium cation binds to the enzyme through the interaction with the delocalized π electrons of three aromatic residues (Tyr60, Trp264, and Trp355) via cation-π bonding, which has recently been reported as unconventional ionic bonding (*54*, *55*). The aromatic residues constitute a so-called aromatic bowl. In DMADH, one of the three aromatic residues (Tyr60) in TMADH is replaced with glutamine (Gln60), and the other residues are conserved (*19*). Dimethylammonium cation may bind to the enzyme via hydrogen bonding between the N−H hydrogen atom of the substrate and the carbonyl group of Gln60 in addition to the cation−π bonding in the active site of DMADH (*22*).

It is noteworthy that the active site structure of HmDH appears to be quite different from that of TMADH. This situation would be responsible for the difference in the substrate selectivity. The putative active site space located at the *si*-face of the isoalloxazine ring (Figure 8a) seems to be more suitable for compounds such as histamine than bulky trimethylamine. In analogy with the previous interaction schemes in TMADH and DMADH, it may be presumed that histamine may bind to HmDH via its protonated amino group as cation−π interaction. In this case, it appears, however, that the protonated amino group does not play a major role because HmDH has no activity toward various aliphatic and aromatic amines. In addition, the protonated amino group of histamine may be directing to Gln64 and Asp357, and the putative catalytic triad (Tyr175, His178, and Asp269) (*41*, *47*, *56*).

The three residues, Trp266, Phe567, and Ser270, might play an important role in the substrate recognition by stabilizing the imidazole moiety via the hydrogen-bond formation with the Ser270 hydroxyl group and π interaction with the aromatic amino acids as seen in several proteins

(*1*). Considering, however, that putrescine and agmatine have protonated amino (p$K_a \cong 9$) and guanidino (p$K_a \cong 12$) groups at optimum pH $\cong$ 8 of HmDH, respectively, these two amines may bind to the enzyme by the interaction with Trp266 and Phe567 via cation$-\pi$ bonding in the same manner as has been proposed in the choline binding site of acetylcholinesterase (*55*). Although the pK_a of imidazole moiety of histamine is about 6.5, this group may be also protonated in the enzyme. The rational site-directed mutagenesis experiments based on sequence alignment study will be helpful for understanding the precise mechanism of the recognition of histamine. In addition, we have recently succeeded in the crystallization of the wild-type HmDH from *N. simplex*, and the crystallographic analysis is on progress. The details may be reported elsewhere soon.

ACKNOWLEDGMENT

We thank Associate Prof. Hirohide Toyama, Department of Biological Chemistry, Yamaguchi University, Japan, for his kind advice in the identification of the *hmd* gene. We also thank Associate Prof. Kazuyoshi Takagi, Department of Science and Technology, Ritsumeikan University, for his help in ESR experiments and for valuable discussions.

REFERENCES

1. Konkimalla, V. B., and Chandra, N. (2003) Determinants of histamine recognition: implications for the design of antihistamines, *Biochem. Biophys. Res. Commun. 309*, 425−431.
2. Siddiqui, J. A., Shoeb, S. M., Takayama, S., Shimizu E., and Yorifuji, T. (2000) Purification and characterization of histamine dehydrogenase from *Nocardioides simplex* IFO 12069, *FEMS Microbiol. Lett. 189*, 183−187.
3. Siddiqui, J. A., Shoeb, S. M., Takayama, S., Shimizu, E., and Yorifuji, T. (2001) Histamine dehydrogenase of *Nocardioides simplex*: a second bacterial enzyme for histamine degradation, *J. Biochem. Mol. Biol. Biophys. 5*, 37−43.
4. Husain, M., and Davidson, V. L. (1987) Purification and properties of methylamine dehydrogenase from *Paracoccus denitrificans*, *J. Bacteriol. 169*, 1712−1717.
5. Iwaki, M., Yagi, T., Horiike, K., Saeki, Y., Ushijima, T., and Nozaki, M. (1983) Crystallization and properties of aromatic amine dehydrogenase from *Pseudomonas* sp., *Arch. Biochem. Biophys. 220*, 253−262.
6. McIntire, W. S., Wemmer, D. E., Chistoserdov, A., and Lidstrom, M. E. (1991) A new cofactor in a prokaryotic enzyme: tryptophan tryptophylquinone as the redox prosthetic group in methylamine dehydrogenase, *Science 252*, 817−824.
7. Govindaraj, S., Eisenstein, E., Jones, L. H., Sanders-Leohr, J., Chistoserdov, A. Y., Davidson, V. L., and Edwards, S. L. (1994) Aromatic amine dehydrogenase, a second tryptophan tryptophylquinone enzyme, *J. Bacteriol. 176*, 2922−2929.
8. Shinagawa, E., Matsushita, K., Nakashima, K., Adachi, O., and Ameyama, M. (1988) Crystallization and properties of amine dehydrogenase from *Pseudomonas* sp., *Agric. Biol. Chem. 52*, 2255−2263.
9. Takagi, K., Torimura, M., Kawaguchi, K., Kano, K., and Ikeda, T. (1999) Biochemical and electrochemical characterization of quinohemoprotein amine dehydrogenase from *Paracoccus denitrificans*, *Biochemistry 38*, 6935−6942.
10. Datta, S., Mori, Y., Takagi, K., Kawaguchi, K., Chen, Z., Okajima, T., Kuroda, S., Ikeda, T., Kano, K., Tanizawa, K., and Mathews, F. S. (2001) Structure of a quinohemoprotein amine dehydrogenase with an uncommon redox cofactor and highly unusual crosslinking, *Proc. Natl. Acad. Sci. U.S.A. 98*, 14268−14273.
11. Satoh, A., Kim, J. K., Miyahara, I., Devreese, B., Vandenberghe, I., Hacisalihoglu, A., Okajima, T., Kuroda, S., Adachi, O., Duine, J. A., Van Beeumen, J., Tanizawa, K., and Hirotsu, K. (2002) Crystal Structure of Quinohemoprotein amine dehydrogenase from *Pseudomonas putida*, *J. Biol. Chem. 277*, 2830−2834.
12. Steenkamp, D. J., and Mallinson, J. (1976) Trimethylamine dehydrogenase from a methylotrophic bacterium. I. Isolation and steady-state kinetics, *Biochim. Biophys. Acta 429*, 705−719.
13. Meiberg, J. B. M., and Harder, W. (1979) Aerobic and anaerobic metabolism of trimethylamine, dimethylamine, and methylamine in *Hyphomicrobium X*, *J. Gen. Microbiol. 115*, 49−58.
14. Hill, C. L., Steenkamp, D. J., Holm, R. H., and Singer, T. P. (1977) Identification of the iron−sulfur center in trimethylamine dehydrogenase, *Proc. Natl. Acad. Sci. U.S.A. 74*, 547−551.
15. Steenkamp, D. J., Kenney, W. C., and Singer, T. P. (1978) A novel type of covalently bound coenzyme in trimethylamine dehydrogenase, *J. Biol. Chem. 253*, 2812−2817.
16. Steenkamp, D. J., McIntire, W., and Kenney, W. C. (1978) Structure of the covalently bound coenzyme of trimethylamine dehydrogenase. Evidence for a 6-substituted flavin, *J. Biol. Chem. 253*, 2818−2824.
17. Steenkamp, D. J. (1979) Identification of the prosthetic groups of dimethylamine dehydrogenase from *Hyphomicrobium X*, *Biochem. Biophys. Res. Commun. 88*, 244−250.
18. Boyd, G., Mathews, F. S., Packman, L. C., and Scrutton, N. S. (1992) Trimethylamine dehydrogenase of bacterium W_3A_1. Molecular cloning, sequence determination, and overexpression of the gene, *FEBS Lett. 308*, 271−276.
19. Yang, C.-C., Packman, L. C., and Scrutton, N. S. (1995) The primary structure of *Hyphomicrobium X* dimethylamine dehydrogenase. Relationship to trimethylamine dehydrogenase and implications for substrate recognition, *Eur. J. Biochem. 232*, 264−271.
20. Lim, L. W., Shamala, N., Mathews, F. S., Steenkamp, D. J., Hamlin, R., and Xuong, N. H. (1986) Three-dimensional structure of the iron−sulfur flavoprotein trimethylamine dehydrogenase at 2.4 Å resolution, *J. Biol. Chem. 261*, 15140−15146.
21. Bellamy, H. D., Lim, L. W., Mathews, F. S., and Dunham, W. R. (1989) Studies of crystalline trimethylamine dehydrogenase in three oxidation states and in the presence of substrate and inhibitor, *J. Biol. Chem. 264*, 11887−11892.
22. Raine, A. R. C., Yang, C.-C., Packman, L. C. White, S. A., Mathews, F. S., and Scrutton, N. S. (1995) Protein recognition of ammonium cations using side-chain aromatics: A structural variation for secondary ammonium ligands, *Protein Sci. 4*, 2625−2628.
23. Basran, J., Mewies, M., Mathews, F. S., and Scrutton, N. S. (1997) Selective modification of alkylammonium ion specificity in trimethylamine dehydrogenase by the rational engineering of cation-π bonding, *Biochemistry 36*, 1989−1998.
24. Inoue, H., Nojima, H., and Okayama, H. (1990) High-efficiency transformation of *Escherichia coli* with plasmids, *Gene 96*, 23−28.
25. Liu, Y.-G., and Whittier, R. F. (1995) Thermal asymmetric interlaced PCR: automatable amplification and sequencing of insert end fragments from P1 and YAC clones for chromosome walking, *Genomics 25*, 674−681.
26. Liu, Y.-G., Mitsukawa, N., Oosumi, T., and Whittier, R. F. (1995) Efficient isolation and mapping of *Arabidopsis thaliana* T-DNA insert junctions by thermal asymmetric interlaced PCR, *Plant J. 8*, 457−463.
27. Hecker, K. H., and Roux, K. H. (1996) High and low annealing temperatures increase both specificity and yield in touchdown and stepdown PCR, *Biotechniques 20*, 478−485.
28. Itzhaki, R. F., and Gill, D. M. (1964) A microbiuret method for estimating proteins, *Anal. Biochem. 9*, 401−410.
29. Massey, V. (1957) Studies on succinic dehydrogenase. VII. Valency state of the iron in beef heart succinic dehydrogenase, *J. Biol. Chem. 229*, 763−770.
30. Chen, J.-S., and Mortenson, L. E. (1977) Inhibition of methylene blue formation during determination of the acid-labile sulfide of iron−sulfur protein samples containing dithionite, *Anal. Biochem. 79*, 157−165.
31. Barber, M. J., Neame, P. J., Lim, L. W., White, S., and Matthews, F. S. (1992) Correlation of X-ray deduced and experimental amino acid sequences of trimethylamine dehydrogenase, *J. Biol. Chem. 267*, 6611−6619.
32. Scrutton, N. S., Packman, L. C., Mathews, F. S., Rohlfs, R. J., and Hille, R. (1994) Assembly of redox centers in the trimethylamine dehydrogenase of Bacterium W_3A_1, *J. Biol. Chem. 269*, 13942−13950.
33. Packman, L. C., Mewies, M., and Scrutton, N. S. (1995) The flavinylation reaction of trimethylamine dehydrogenase, *J. Biol. Chem. 270*, 13186−13191.

34. Mewies, M., Packman, L. C., Mathews, F. S., and Scrutton, N. S. (1996) Flavinylation in wild-type trimethylamine dehydrogenase and differentially charged mutant enzymes: a study of the protein environment around the N1 of the flavin isoalloxazine, *Biochem. J. 317*, 267−272.
35. Mewies, M., McIntire, W. S., and Scrutton, N. S. (1998) Covalent attachment of flavin adenine dinucleotide (FAD) and flavin mononucleotide (FMN) to enzymes: the current state of affairs, *Protein Sci. 7*, 7−20.
36. Edmondson, D. E., and Singer, T. P. (1973) Oxidation−reduction properties of the 8α-substituted flavins, *J. Biol. Chem. 248*, 8144−8149.
37. Steenkamp, D. J., and Singer, T. P. (1978) Participation of the iron−sulphur cluster and of the covalently bound coenzyme of trimethylamine dehydrogenase in catalysis, *Biochem. J. 169*, 361−369.
38. Steenkamp, D. J., and Beinert, H. (1982) Mechanistic studies on the dehydrogenases of methylotrophic bacteria. 1. The influence of substrate binding to reduced trimethylamine dehydrogenase on the intramolecular electron transfer between its prosthetic groups, *Biochem. J. 207*, 233−239.
39. Kasprzak, A. A., Papas, E. J., and Steenkamp, D. J. (1983) Identity of the subunits and the stoichiometry of prosthetic groups in trimethylamine dehydrogenase and dimethylamine dehydrogenase, *Biochem. J. 211*, 535−541.
40. Basran, J., Jang, M. H., Sutcliffe, M. J., Hille, R., and Scrutton, N. S. (1999) The role of Tyr-169 of trimethylamine dehydrogenase in substrate oxidation and magnetic interaction between FMN cofactor and the 4Fe/4S center, *J. Biol. Chem. 274*, 13155−13161.
41. Basran, J., Sutcliffe, M. J., and Scrutton, N. S. (2001) Optimizing the Michaelis complex of trimethylamine dehydrogenase, *J. Biol. Chem. 276*, 42887−42892.
42. Guex, N., and Peitsch, M. C. (1997) SWISS-MODEL and the Swiss-PdbViewer: an environment for comparative protein modeling, *Electrophoresis 18*, 2714−2723.
43. Kraulis, P. J. (1991) MOLSCRIPT: a program to produce both detailed and schematic plots of protein structures, *J. Appl. Crystallogr. 26*, 283−291.
44. Steenkamp, D. J., and Beinert, H. (1982) Mechanistic studies on the dehydrogenases of methylotrophic bacteria. 2. Kinetic studies on the intramolecular electron transfer in trimethylamine and dimethylamine dehydrogenase, *Biochem. J. 207*, 241−245.
45. Stevenson, R. C., Dunham, W. R., Sands, R. H., Singer, T. P., and Beinert, H. (1986) Studies on the spin−spin interaction between flavin and iron−sulfur cluster in an iron−sulfur flavoprotein, *Biochim. Biophys. Acta 869*, 81−88.
46. Fournel, A., Gambarelli, S., Guigliarelli, B., More, C. Asso, M., Chouteau, G., Hille, R., and Bertrand, P. (1998) Magnetic interactions between a $[4Fe-4S]^{1+}$ cluster and a flavin mononucleotide radical in the enzyme trimethylamine dehydrogenase: A high-field electron paramagnetic resonance study, *J. Chem. Phys. 109*, 10905−10913.
47. Jang, M. H., Basran, J., Scrutton, N. S., and Hille, R. (1999) The reaction of trimethylamine dehydrogenase with trimethylamine, *J. Biol. Chem. 274*, 13147−13154.
48. Steenkamp, D. J., and Gallup, M. (1978) The natural flavoprotein electron acceptor of trimethylamine dehydrogenase, *J. Biol. Chem. 253*, 4086−4089.
49. Wilson, E. K., Mathews, F. S., Packman, L. C., and Scrutton, N. S. (1995) Electron tunneling in substrate-reduced trimethylamine dehydrogenase: Kinetics of electron transfer and analysis of the tunneling pathway, *Biochemistry 34*, 2584−25891.
50. Wilson, E. K., Huang, L., Sutcliffe, M. J., Mathews, F. S., Hille, R., and Scrutton, N. S. (1997) An exposed tyrosine on the surface of trimethylamine dehydrogenase facilitates electron transfer to electron transferring flavoprotein: Kinetics of transfer in wild-type and mutant complexes, *Biochemistry 36*, 41−48.
51. Basran, J., Chohan, K. K., Sutcliffe, M. J., and Scrutton, N. S. (2000) Differential coupling through Val-344 and Tyr-442 of trimethylamine dehydrogenase in electron-transfer reactions with ferricenium ions and electron transferring flavoprotein, *Biochemistry 39*, 9188−9200.
52. Leys, D., Basran, J., Talfournier, F., Sutcliffe, M. J., and Scrutton, N. S. (2003) Extensive conformational sampling in a ternary electron-transfer complex, *Nat. Struct. Biol. 10*, 219−225.
53. Ebert, S., Rieger, P.-G., and Knackmuss, H.-J. (1999) Function of coenzyme F420 in aerobic catabolism of 2,4,6-trinitrophenol and 2,4-dinitrophenol by *Nocardioides simplex* FJ2-1A, *J. Bacteriol. 181*, 2669−2674.
54. Deakyne, C. A., and Meot-Ner, M. (1985) Unconventional ionic hydrogen bonds. 2. $NH^{+}\cdots\pi$. Complexes of onium ions with olefins and benzene derivatives, *J. Am. Chem. Soc. 107*, 474−479.
55. Scrutton, N. S., and Raine, A. R. C. (1996) Cation-π bonding and amino-aromatic interactions in the biomolecular recognition of substituted ammonium ligands, *Biochem. J. 319*, 1−8.
56. Basran, J., Sutcliffe, M. J., Hille, R., and Scrutton, N. S. (1999) Reductive half-reaction of the H172Q mutant of trimethylamine dehydrogenase: evidence against a carbanion mechanism and assignment of kinetically influential ionizations in the enzyme−substrate complex, *Biochem. J. 341*, 307−314.

BI049061Q